p-ISSN: 2301-6663, e-ISSN: 2477-250X
URL: http://ojs.ummetro.ac.id/index.php/turbo

THE EFFECT OF OFFSET RATIO ON OFFSET JET FLOW STRUCTURE

Rifqi Ramadhani[1], James Julian[1*], Fitri Wahyuni[1], Riki Hendra Purba[1], Fathin Muhammad Mahdhudhu[2], Elvi Armadani[3]

[1]Department of Mechanical Engineering, Universitas Pembangunan Nasional Veteran Jakarta Jln. RS. Fatmawati Raya. Pd. Labu, Kec. Cilandak, Kota Depok, Jawa Barat 12450, Indonesia
[2]Department of Naval Architecture, Universitas Pembangunan Nasional Veteran Jakarta Jln. RS. Fatmawati Raya. Pd. Labu, Kec. Cilandak, Kota Depok, Jawa Barat 12450, Indonesia
[3]Department of Industrial Engineering, Universitas Pembangunan Nasional Veteran Jakarta Jln. RS. Fatmawati Raya. Pd. Labu, Kec. Cilandak, Kota Depok, Jawa Barat 12450, Indonesia
**Corresponding author*: zames@upnvj.ac.id

Abstract

Jet flow is a fundamental fluid-dynamics phenomenon that has been extensively studied. This phenomenon plays a crucial role in various industrial applications, including surface cleaning, flow control, and cooling of electronic components. Offset jets offer advantages in flow pattern control by expanding the impingement area and regulating surface pressure distribution. However, the aerodynamic behavior associated with a single offset jet at low offset ratios has not been explored in depth. Therefore, this study aims to investigate the effect of varying offset jet ratios on the aerodynamic characteristics of a single offset jet, focusing on impingement zone formation, pressure distribution, and surface shear behavior. This study uses Computational Fluid Dynamics (CFD) to investigate the effects of variations in jet offset ratio on the flow's aerodynamic characteristics. This study used a standard k-ε turbulence model with a structured mesh and a Reynolds number of 10,000. The mesh element used was a fine mesh with 200,000 elements and an error percentage of 0.09436%. The results showed that an OR 3 produced the highest C_f value of 0.0047, a stable Cp distribution of 0.218, and the best impingement zone area.
Keywords**:** *Computational fluid dynamic, Impinging zone, Offset jet, Offset ratio, Pressure*.

1. Introduction

(Jet flow is a crucial phenomenon in fluid dynamics that is widely applied in various engineering systems, including surface cleaning, flow control, and precision cooling processes, such as cooling electronic components [1–4]. One commonly used configuration is the impinging jet, where the fluid flow is directed perpendicular to the target surface, creating an impingement zone that is typically used to maximize momentum and heat transfer [5]. However, this model has limitations; the increase in surface pressure is too high and centralized, which has the potential to damage the target surface [6]. To overcome these limitations, the offset jet configuration offers several advantages, including reduced local pressure on the surface and an expanded impingement zone [7]. The jet flow works by adjusting the flow direction through the offset height parallel to the target surface, thus producing a flow pattern that is directly deflected towards the surface [8].

The promising potential of the offset jet configuration has attracted the attention of many researchers to study the characteristics of the flow structure in various applicable fields. A study comprehensively examines the behavior of offset jets in a dual-jet configuration using the particle image velocimetry (PIV) approach [9]. The study describes the visualization of the jet flow field at an offset ratio (d/w) = 1 and Reynolds number (Re) = 10000. The visualization results reveal a large-scale, periodic Karman-like vortex shedding phenomenon resulting from the interaction between the two jets. This phenomenon affects both the free shear layer of the offset jet and the wall boundary layer of the wall jet. However, the study focused on one offset configuration without considering operational parameters.

Furthermore, another study

DOI: http://dx.doi.org/10.24127/trb.v14i2.4538
Received September 03, 2025; Received in revised form December 26, 2025; Accepted December 28, 2025
Available online December 31, 2025

investigates several operational parameters that quantitatively affect the flow field in a dual jet configuration [10]. An increase in the velocity ratio (r) can shift the merge point upstream by up to 41.5% at an offset ratio H = 15. In addition, further studies were conducted by adding ejection angle parameters that specifically reduced the axial position of the upper vortex center (UVC) by up to 53.9% [11]. In addition, two other studies focused on examining the flow field characteristics in single and dual offset jet configurations [12,13]. The research results showed that the addition of a wall jet in a single offset jet (SOJ) configuration weakened the recirculation zone, as evidenced by a higher minimum static pressure value and lower backflow velocity. Meanwhile, exploration of the dual offset jet (DOJ) configuration revealed fundamental structural differences, including the formation of two recirculation zones.

Although offset jet flow has been extensively investigated and has shown continuous development, existing studies are predominantly focused on configurations with relatively high offset ratios. As a result, the fundamental flow structures and aerodynamic characteristics of single-offset jets at low offset ratios remain underexplored. This limitation is critical, as the offset ratio plays a key role in governing fluid–surface interaction, impingement zone formation, and momentum redistribution, which are essential for effective flow control in precision engineering applications. Therefore, this study aims to systematically investigate the influence of variations in the low offset ratio on the aerodynamic characteristics of a single offset jet at a Reynolds number of 10,000. The variations OR range from OR 1 to 5, with an interval of 0.5. The results of this study are expected to lay the foundation for future research on single offset jets with low ratios and to address the knowledge gap regarding the aerodynamic behavior in offset jet flows.

2. Methodology

2.1 Offset Jet Configuration

This study was conducted to analyze the offset jet flow phenomenon in a two-dimensional configuration. The operational factors studied indicate that the intensity of the influence of 3-dimensional (3D) flow is minimal, allowing the influence of the 3D mode perspective to be ignored [7]. Additionally, the two-dimensional approach substantially enhances the efficiency of computational calculations without significantly compromising the accuracy of the results. The geometry configuration of the offset jet is shown in Figure 1. The offset jet flow is divided into three main zones, namely: 1) pre-impingement zone, 2) impingement zone, and 3) wall jet region.

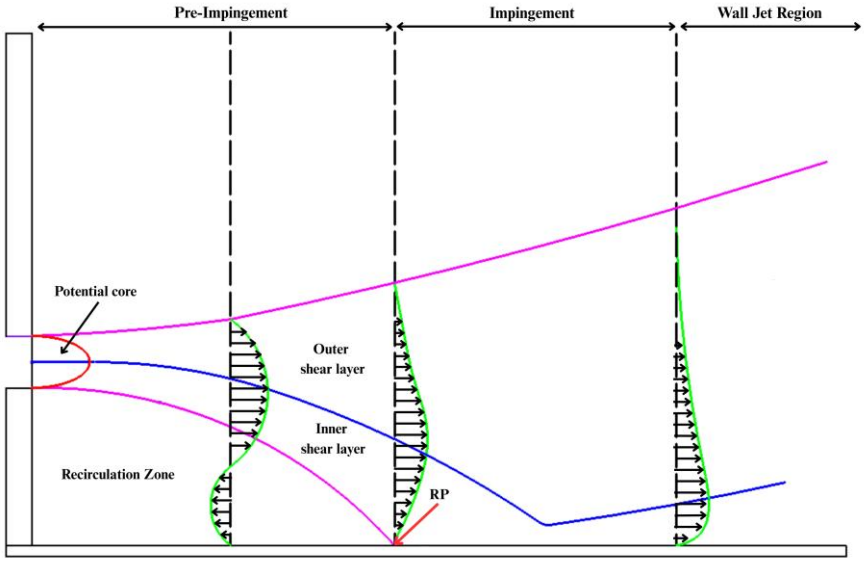

Figure 1. Offset jet region

2.2 Governing equations.

This research uses OpenFOAM, an open-source software, to solve CFD cases.

The Reynolds-averaged Navier-Stokes (RANS) equation is essential to CFD. It has two main components: the continuity and momentum equations. These have been adjusted to solve fluid dynamics problems in CFD applications. Formally, the RANS expression is written as an equation (1) and (2) [14].

$$\frac{\partial \rho}{\partial t} + \frac{\partial}{\partial x_i}(\rho u_i) = 0 \quad (1)$$

$$\frac{\partial}{\partial t}(\rho u_i) + \frac{\partial}{\partial x_i}(\rho u_i u_j) = \frac{\partial p}{\partial x_i} + \frac{\partial}{\partial x_j} \quad (2)$$

$$\left[\mu\left(\frac{\partial u_i}{\partial x_j} + \frac{\partial u_j}{\partial x_i} - \frac{2}{3}\delta_{ij}\frac{\partial u_i}{\partial x_i}\right) \right] +$$

$$\frac{\partial}{\partial x_i}(-\rho\overline{u'_i u'_j})$$

$$\frac{\partial}{\partial t}(\rho k) = \frac{\partial}{\partial x_j}\left[(\mu + \frac{\mu_t}{\sigma_k})\frac{\partial k}{\partial x_j} \right] \quad (3)$$

$$+G_k - \rho\varepsilon$$

$$\frac{\partial}{\partial t}(\rho\varepsilon) = \frac{\partial}{\partial x_j}\left[(\mu + \frac{\mu_t}{\sigma_\varepsilon})\frac{\partial \varepsilon}{\partial x_j} \right] + \quad (4)$$

$$C_{e1}\frac{\varepsilon}{k}G_k - \rho C_{\varepsilon 2}\frac{\varepsilon^2}{k}$$

A turbulence model is necessary to complete the calculation more accurately and predict complex turbulent fluid flows. This study uses the model standard k-ε, it includes the turbulent kinetic energy (k) in Equation (3) and dissipation rate (ε) in Equation (4) [15]. The standard k-ε model is most commonly used because it is accurate in predicting the offset jet flow field phenomenon [13,16].

2.3 Mesh and Boundary Conditon

Mesh creation is crucial for ensuring accuracy in numerical calculations. As shown in Figure 2 (a), a quadrilateral structured mesh was implemented to ensure accurate computational results, particularly for fluid interactions with solid surfaces. The fluid enters the domain with a calm environment, set at U=1 and V=0 and the Reynolds number as 10,000 described in Equation (5).

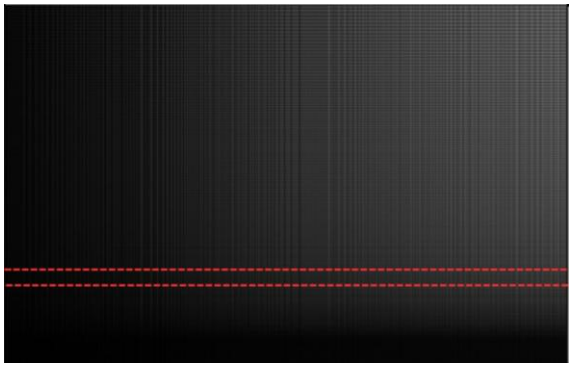

(a)

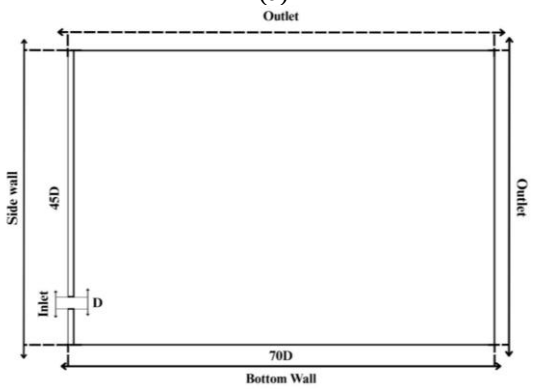

(b)

Figure 2. Detail of mesh and boundary condition (a) Mesh and (b) Boundary Condition

$$\mathrm{Re} = \frac{\rho D V}{\mu} \quad (5)$$

Furthermore, the exit is configured as a zero-pressure outlet. Additionally, the boundary conditions for the walls are set to no-slip. More detail about the boundary condition and the domain of computational can be seen in Figure 2 (b). This computational domain has nozzles of size D. The total area of the computational domain is $70D \times 50D$. This study analyzes the effect of OR on the offset jet. The offset ratio variation used is offset ratio (OR) 1 to 5. The variations in this research are shown in Table 1 in detail. The convergence criteria for each variable, as determined in this study, are 10^{-6}.

Table 1. Parameter geometry and the offset ratio

Parameters	Value
Diameter (D)	10 mm
Bottom wall	700 mm
Side wall	450 mm
Offset ratio (OR)	1; 1.5; 2; 2.5; 3; 3.5; 4; 4.5; 5

2.4 Friction Coefficient

The friction coefficient (C_f) is defined as a non-dimensional number of parameters that occurred between the fluid and the surface of a solid object [17]. This phenomenon is observed when the friction effect appears due to the interaction of the fluid with the solid surface, representing the viscosity zone. In the case of jet flow, this phenomenon is essential to confirm that the fluid is not inviscid. Furthermore, the representation of this phenomenon constructs a boundary layer that continuously grows, leading to a significant transformation of the velocity gradient in the fluid flow. Mathematically, C_f is formulated in Equation (6).

$$C_f = \frac{\tau_w}{\frac{1}{2}\rho U^2} \tag{6}$$

2.5 Mesh Independence test

This analysis employs a structured mesh consisting of quadrilateral elements. The mesh variation is determined by the element count, which includes fine, medium, and coarse meshes. The mesh elements count is 200,000, 100,000, and 50,000, respectively. The test is conducted using the method proposed by Roache [18]. This method is designed to quantify the uncertainties and errors introduced by the spatial discretization process. Before performing the mesh independence test, specific variable samples must be obtained for each mesh type. For this study, the fluid velocity is set at coordinates X = 0.3 and Y = 0.025 for comparison data. There are several main steps in this test. First step is to determine the amount of mesh variation ratio using Equation (8). After that, the mesh convergence order calculation is carried out with the Equation (9). The third step involves determining the deviation for each mesh variation by calculating the grid convergence index (GCI) using Equations (10) and (11). The GCI_{fine} determines the amount of error found in the fine and medium meshes [19]. Meanwhile, GCI_{coarse} is used to measure the deviation between the medium and coarse meshes. The GCI calculation results are then used to ensure the three mesh variations are in the convergent area. After completing all calculation stages, the lowest error value is obtained with the fine mesh at 0.09436%, as shown in Figure 2. Based on these results, the fine mesh is determined to be the optimal resolution for numerical simulations, providing more accurate and convergent results.

$$r = \frac{h_2}{h_1} \tag{8}$$

$$\bar{p} = \frac{\ln\left(\frac{f_3 - f_2}{f_2 - f_1}\right)}{\ln(r)} \tag{9}$$

$$GCI_{fine} = \frac{F_s |\varepsilon|}{\left(r^{\bar{p}} - 1\right)} \tag{10}$$

$$GCI_{coarse} = \frac{F_s |\varepsilon| r^{\bar{p}}}{\left(r^{\bar{p}} - 1\right)} \tag{11}$$

$$\varepsilon = \frac{f_{n+1} - f_n}{f_n} \tag{12}$$

$$\frac{GCI_{coarse}}{GCI_{fine}} \approx 1 \tag{13}$$

$$fr_{h=0} = f_1 + \frac{(f_1 - f_2)}{\left(r^{\bar{p}} - 1\right)} \tag{14}$$

Tabel 2. Grid test results

Mesh	Fine	Medium	Coarse
Velocity	5.441548	5.437274	5.429448
$\bar{p}$		0.87295897	
r		2	
GCI_{fine}		0.118%	
GCI_{coarse}		0.2164%	
$\frac{GCI_{coarse}}{GCI_{fine}\, r^{\bar{p}}}$		1	
Error	0.09436%	0.71282%	0.31650%

3. Result and Discussion

3.1 Validation

This research employed a computational approach to more efficiently model offset jet flow than an experimental approach. However, numerical calculations are limited in their ability to represent actual field conditions due to model assumptions

and simplifications. Therefore, validating the numerical results is essential to achieving accurate simulations. Validation was performed by comparing the results of numerical calculations with experimental data [20] and the previous study with jet offset configurations having an offset ratio (OR) of 2.5.

The average error of the current study's U_{decay} relative to experimental data is approximately 4%. The u-decay trend graph in Figure 3 shows good agreement with experimental results, although there are minor differences in the pre-impingement and downstream regions. A comparison with previous studies using a similar turbulence model reveals that the current simulation yields a trend closer to the experimental results. Overall, these validation results suggest that the numerical simulation accurately represents the primary characteristics of the offset jet flow within acceptable limits, making it suitable for further analysis of the effects of low OR variations on the offset jet flow behavior.

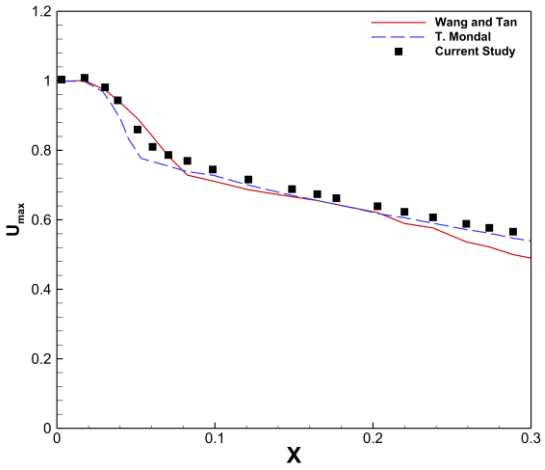

Figure 3. U_{decay} Comparison between numerical and experimental study

3.2 Analysis.

This investigation examines how variations in the jet offset ratio affect the impingement zone in a flow with Re 10,000.

Figure 4 presents the variation of the maximum velocity decay (U_{decay}) along the streamwise direction for different offset ratios. Upon exiting the nozzle, the jet initially maintains its maximum velocity within a potential core region, consistent with classical free jet theory [21]**.** Beyond this region, velocity decay occurs due to momentum diffusion and entrainment of the surrounding fluid. At low offset ratios, Umax decays more rapidly in the upstream region. This behavior is attributed to the proximity between the nozzle and the bottom wall, which promotes early jet–wall interaction and accelerates the breakdown of the potential core. In contrast, higher offset ratios provide sufficient vertical clearance for the jet to develop a more stable potential core before interacting with the wall, leading to slower upstream velocity decay.

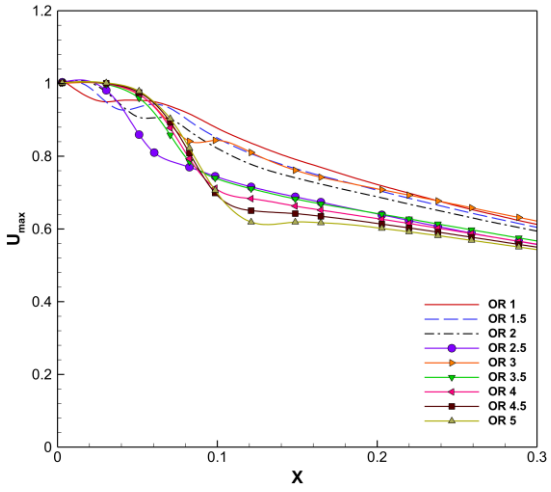

Figure 1. U_{decay} variations at each offset ratio

However, in the downstream region, higher offset ratios exhibit a more pronounced velocity reduction compared to lower OR cases. This phenomenon is caused by the enlargement of the recirculation zone beneath the jet, which dissipates jet momentum through vortex-induced mixing before reattachment occurs. Consequently, although higher OR configurations preserve the jet velocity upstream, they experience greater momentum loss downstream due to increased recirculation.

The variation in the offset ratio was shown to affect the velocity drop in the jet stream significantly. The greater the velocity drop, the more intense the momentum transfer process is before finally hitting the bottom wall (reattachment point), forming an impingement zone. Figure 5 shows the location and characteristics of the

reattachment point with respect to the X position.

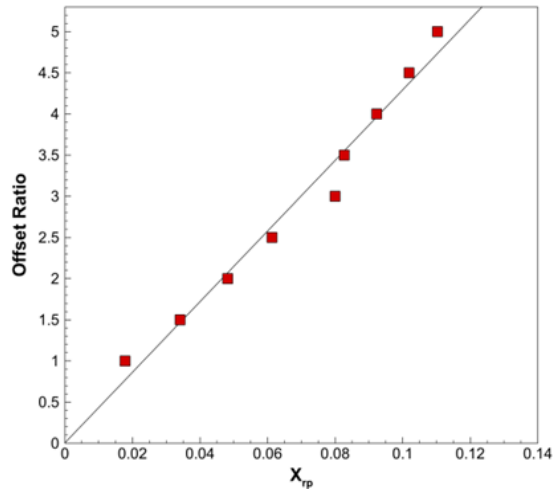

Figure 5. X_{rp} location at each offset ratio

The graph shows that the positions of the reattachment points increase with the offset ratio. The X_{rp} is one of the critical locations in the jet flow phenomenon where the fluid hits the wall before finally flowing along the wall surface. The offset ratio plays a significant role in determining the location and characteristics of the X_{rp}. At lower offset ratios, the jet stream will reattach more quickly than at higher ones. The formation of a larger recirculation zone just below the nozzle is the reason for this [22].

In jet studies, variations of the Coefficient of Friction (C_f) and Coefficient of Pressure (C_p) are shown to investigate the jet flow field's characteristics interacting with the bottom wall. The skin friction coefficient is used to characterize wall shear stress and to identify reattachment behavior. C_f is an important parameter, especially when determining the position of the reattachment point or the local location of impingement zone formation. Figure 6 shows that C_f approaches zero near the reattachment point, which is a well-known indicator of flow reversal and the location of reattachment point [16].

An increase in OR indicates a shift in the X_{rp} towards downstream. Therefore, this finding is directly proportional to the size of the recirculation zone formed. In addition, the C_f value increases due to the formation of the impingement zone. Computational results indicate that the jet interaction of the jet stream with the surface is most dominant at OR 3. Among all configurations, OR 3 exhibits the highest peak C_f value of 0.0047, indicating the strongest wall shear stress and momentum transfer. This result suggests that OR 3 provides an optimal balance between jet momentum and recirculation size, allowing the jet to impinge effectively without excessive energy dissipation. Both lower and higher OR values result in reduced C_f peaks, either due to premature jet–wall interaction (low OR) or excessive momentum loss within the recirculation zone (high OR).

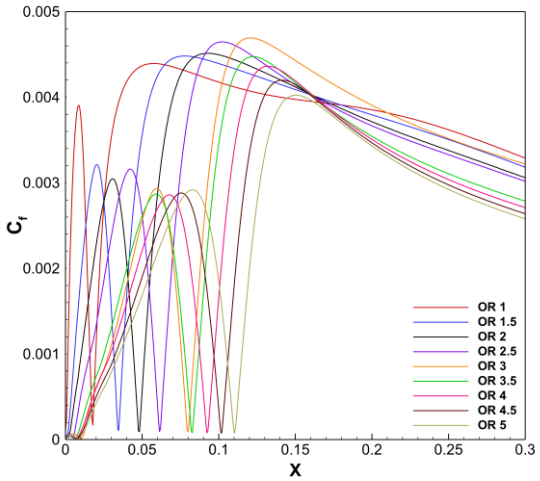

Figure 6. C_f variations at various offset ratio

Moreover, Figure 7 illustrates the coefficient of pressure (C_p) to provide a more comprehensive depiction of the flow field interactions at the bottom wall. The C_p curve exhibits two main features: a recirculation zone and a stagnation pressure at the reattachment site. A negative-pressure field characterizes the recirculation zone resulting from flow separation from the bottom wall**.** On the other hand, the peak value in C_p indicates the reattachment location of the jet stream. Increasing the offset ratio significantly increases the peak C_p value at the bottom wall. OR 5 significantly dominates the pressure field at the bottom wall with a value of 0.2426. This is due to the high offset ratio that allows the fluid velocity vector to deflect in the

negative y direction. Therefore, the jet stream collision can occur over a larger frontal area.

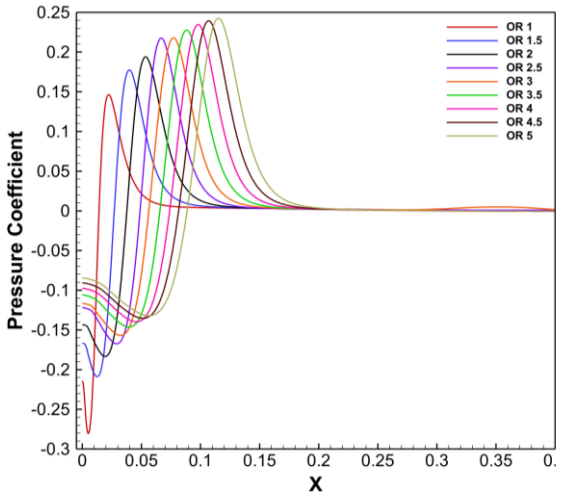

Figure 7 C_p variations at various offset ratio

Table 3 quantitatively confirms that increasing OR shifts X_{rp} downstream while simultaneously increasing $C_{p,max}$ and reducing the magnitude of $C_{p,min}$. This trend indicates that higher offset ratios weaken flow separation intensity but enhance pressure recovery at the impingement location[16].

Table 3. Characteristic of X_{rp}

OR	X_{rp}	$C_{p,min}$	$C_{p,max}$
1	0.0178	-0.2807	0.1466
1.5	0.0341	-0.2089	0.1776
2	0.0482	-0.1834	0.194
2.5	0.0613	-0.1675	0.2176
3	0.08	-0.1569	0.218
3.5	0.0827	-0.1463	0.2277
4	0.0923	-0.1398	0.2346
4.5	0.1019	-0.1354	0.2394
5	0.1103	-0.1321	0.2426

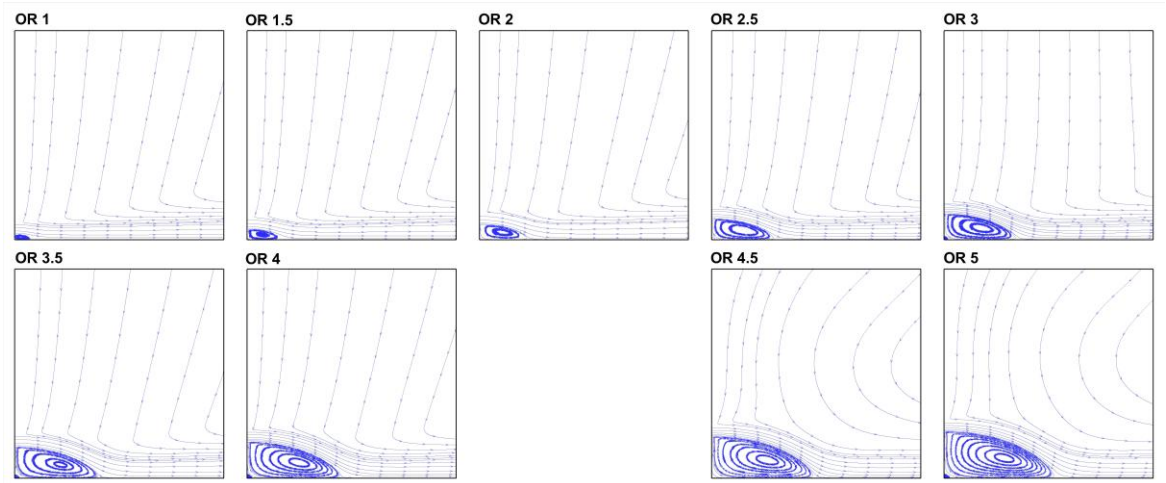

Figure 8. Streamline contour

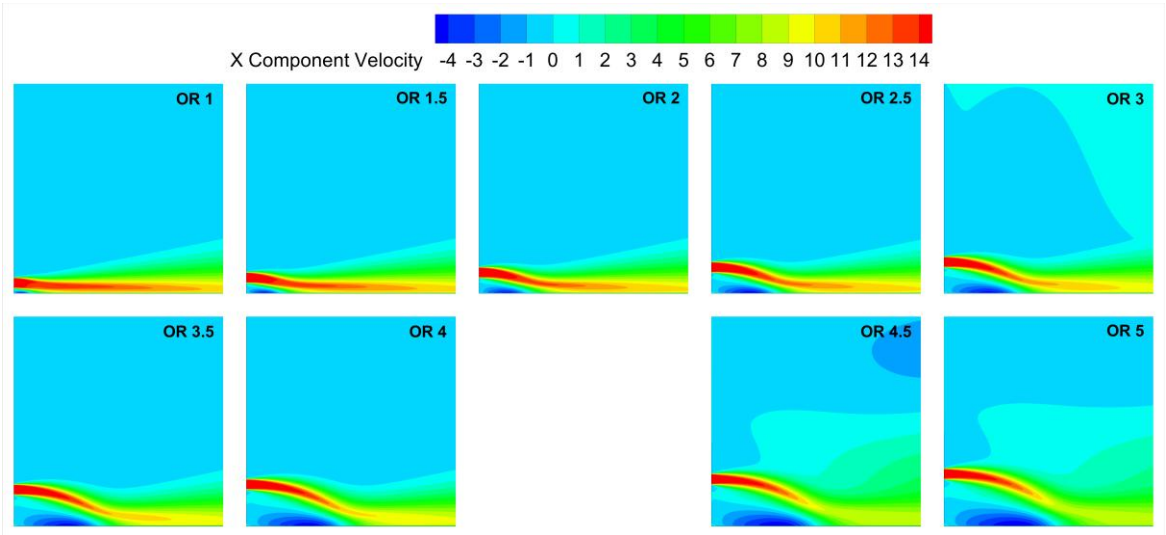

Figure 9. Velocity contour

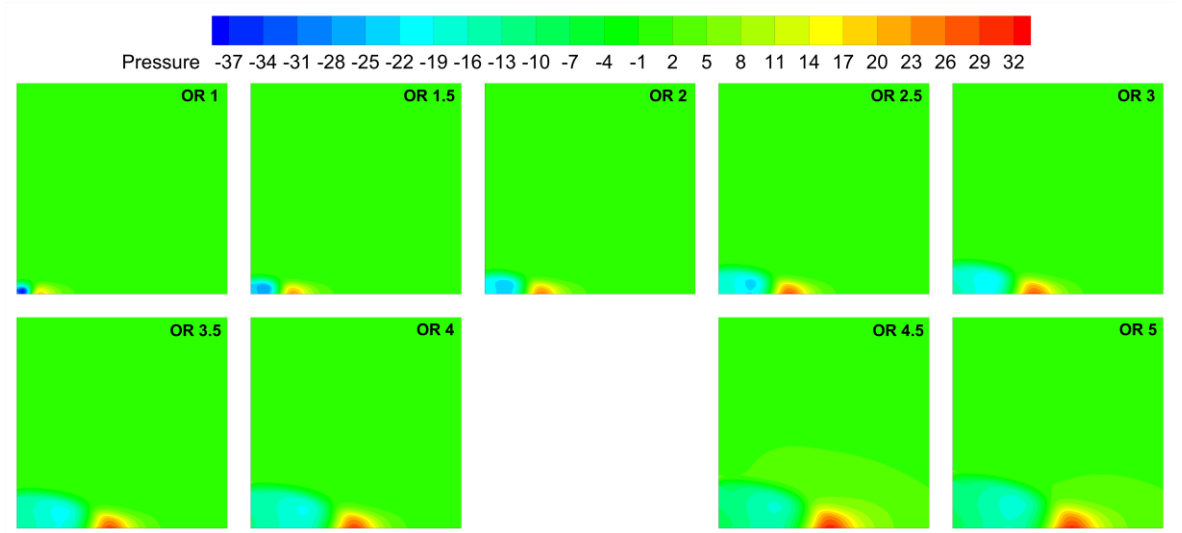

Figure 10. Pressure contour

The shifted X_{rp} indicates that the jet stream has a longer path before interacting with the bottom wall due to the dominance of the recirculation zone. For the pressure coefficient, $C_{p,max}$ is 0.2426 at an offset ratio of 5, while $C_{p,min}$ is 0.1466 at an offset ratio of 1. The most significant increase in value occurs at OR 1.5 compared with OR 1, with a difference of 0.031. Meanwhile, the lowest $C_{p,min}$ value is -0.2807 at OR 1, and the highest $C_{p,min}$ value is at OR 5 with a value of -0.1321.

Figure 8 illustrates the streamline patterns for each offset ratio, showing that the jet deflects toward the bottom wall and attaches to the surface due to the Coanda effect [22]**.** This attachment results from entrainment-induced pressure differences that cause the jet to follow the nearby wall, forming a wall-jet structure with a recirculation zone beneath the jet. As the offset ratio increases, the recirculation zone becomes larger. At OR 1 and OR 1.5, the limited nozzle-to-wall distance suppresses vortex development, and no secondary vortex is observed at the corner between the vertical wall and the bottom wall. In contrast, Figure 9 shows that for OR ≥ 2, a secondary vortex begins to form due to enhanced shear-layer development and increased flow separation. The enlargement of the recirculation region shifts the reattachment point further downstream, delaying jet–wall interaction.

This flow behavior is consistent with the surface pressure distribution shown in Figure 10. From the perspective of Bernoulli's principle, the deceleration and redirection of the jet during reattachment convert kinetic energy into static pressure [16]. Higher offset ratios allow the jet to reattach more frontally, enhancing momentum transfer to the wall and increasing surface pressure. These results confirm that the offset ratio strongly governs vortex formation, reattachment location, and surface pressure characteristics in single offset jet flows, making it a key parameter for controlling impingement behavior in precision flow applications.

4. Conclusion

This study analyzes the impact of jet OR variations on the characteristics of the impingement zone at a Reynolds number of 10,000 within the OR range of 1 to 5, with an interval of 0.5. Simulation results indicate that the OR has a significant impact on pressure distribution, impingement zone, recirculation zone, and reattachment distance. The study has limitations: 2D, the standard k-ε turbulence model, and the assumption of incompressible flow. It focuses on the aerodynamic characteristics

of jet flow without involving thermal parameter analysis.

Due to its proximity to the wall, the highest U_{max} drop gradient occurs at an offset ratio 1. As the offset ratio increases, the U_{max} drop can be reduced as a flow phenomenon that maintains momentum. However, due to increasing the jet height, the velocity drop is more significant compared to the low offset ratio. Furthermore, the reattachment point distance on OR 5 increased tenfold from the reattachment distance on OR 1, with respective values of X_{rp} 0.1103 and 0.0178. It can be concluded that X_{rp} the distance increases as the offset ratio rises. Furthermore, the maximum C_f value is obtained at OR 3, which is 0.0047. The variation in OR 3 is considered the most effective offset ratio parameter in forming the impingement zone, as indicated by the peak C_f value. On the other hand, an increase in the offset ratio significantly affects the peak C_p value on the lower surface. OR 5 significantly dominates the pressure field on the surface with a value of 0.2426, and the C_p value decreases as the OR value decreases.

The results of this study indicate that the OR 3 configuration has the best impingement zone, as seen from the high interaction between the fluid and the surface. This configuration yields a stable surface pressure compared to other OR configurations. The results of this study have the potential to be applied to precision systems, such as electronic component cooling, surface drying processes, and precision cleaning in the manufacturing industry. In the future, this research can be expanded to include thermal parameter analysis, such as temperature distribution and Nusselt number, to obtain a comprehensive understanding of heat transfer performance. This study will not only enrich the scientific understanding of offset jet characteristics but also provide a stronger foundation for design optimization in various industrial applications that require efficient momentum and heat transfer.

Reference

[1] Sarkar S, Gupta R, Roy T, Ganguly R, Megaridis CM. Review of jet impingement cooling of electronic devices: Emerging role of surface engineering. Int J Heat Mass Transf 2023;206. https://doi.org/10.1016/j.ijheatmasstransfer.2023.123888.

[2] Zhang Y, Zhou Z, Wang K, Li X. Aerodynamic characteristics of different airfoils under varied turbulence intensities at low Reynolds numbers. Applied Sciences (Switzerland) 2020;10. https://doi.org/10.3390/app10051706.

[3] Wei T, Oprins H, Cherman V, Beyne E, Baelmans M. Low-Cost Energy-Efficient On-Chip Hotspot Targeted Microjet Cooling for High- Power Electronics. IEEE Trans Compon Packaging Manuf Technol 2020;10:577–89. https://doi.org/10.1109/TCPMT.2019.2948522.

[4] Ruan D, Cheng Y, Hou J, Xue S, Yang S, Ma X. Mass transfer and mixing performance in jet-to-counterflow micromixer. Chemical Engineering Journal 2024;498. https://doi.org/10.1016/j.cej.2024.155348.

[5] Mishra A, Yadav H, Djenidi L, Agrawal A. Experimental study of flow characteristics of an oblique impinging jet. Exp Fluids 2020;61. https://doi.org/10.1007/s00348-020-2923-y.

[6] Khalil MF, Elshorbagy KA, Kassab SZ, Elmiligui AA. Experimental and numerical parametric study of the plane- offset jet impinging on a flat surface. 35th AIAA Fluid Dynamics Conference and Exhibit, 2005. https://doi.org/10.2514/6.2005-5012.

[7] Assoudi A, Habli S, Saïd NM, Bournot P, Palec G Le. Numerical study of a turbulent offset jet flow. Lecture Notes in Mechanical

Engineering 2015;789:703–11. https://doi.org/10.1007/978-3-319-17527-0_70.
[8] Kumar A. Mean flow characteristics of a turbulent dual jet consisting of a plane wall jet and a parallel offset jet. Comput Fluids 2015;114:48–65. https://doi.org/10.1016/j.compfluid.2015.02.017.
[9] Wang XK, Tan SK. Experimental investigation of the interaction between a plane wall jet and a parallel offset jet. Exp Fluids 2007;42:551–62. https://doi.org/10.1007/s00348-007-0263-9.
[10] Hnaien N, Marzouk S, Aissia H Ben, Jay J. Numerical investigation of velocity ratio effect in combined wall and offset jet flows. Journal of Hydrodynamics 2018;30:1105–19. https://doi.org/10.1007/s42241-018-0136-0.
[11] Hnaien N, Marzouk S, Kolsi L, Alsagri AS, Ben Aissia H, Jay J. Offset jet ejection angle effect in combined wall and offset jets flow: numerical investigation and engineering correlations. Journal of the Brazilian Society of Mechanical Sciences and Engineering 2019;41. https://doi.org/10.1007/s40430-019-1982-6.
[12] Assoudi A, Mahjoub Saïd N, Bournot H, Le Palec G. Comparative study of flow characteristics of a single offset jet and a turbulent dual jet. Heat and Mass Transfer/Waerme- Und Stoffuebertragung 2019;55:1109–31. https://doi.org/10.1007/s00231-018-2493-1.
[13] Mondal T, Srivastava N, O'Shaughnessy SM, Pramanik S. Comparison of the mean flow and turbulence characteristics of a single offset jet and a dual offset jet. European Journal of Mechanics, B/Fluids 2023;98:161–79. https://doi.org/10.1016/j.euromechflu.2022.12.003.
[14] Singh TP, Kumar A, Satapathy AK. Fluid flow analysis of a turbulent offset jet impinging on a wavy wall surface. Proc Inst Mech Eng C J Mech Eng Sci 2020;234:544–63. https://doi.org/10.1177/0954406219880209.
[15] Julian J, Iskandar W, Wahyuni F, Armansyah A, Ferdyanto F. Effect of Single Slat and Double Slat on Aerodynamic Performance of NACA 4415. International Journal of Marine Engineering Innovation and Research 2022;7. https://doi.org/10.12962/j25481479.v7i2.12875.
[16] Mondal T, Pramanik S. Numerical study on mean flow field of turbulent dual offset jet. Proc Inst Mech Eng C J Mech Eng Sci 2021;235:6865–82. https://doi.org/10.1177/0954406221100077 4.
[17] Julian J, Iskandar W, Wahyuni F. COMPUTATIONAL FLUID DYNAMICS ANALYSIS BASED ON THE FLUID FLOW SEPARATION POINT ON THE UPPER SIDE OF THE NACA 0015 AIRFOIL WITH THE COEFFICIENT OF FRICTION. Jurnal Media Mesin n.d.;23.
[18] Roache PJ. Perspective: A Method for Uniform Reporting of Grid Refinement Studies. 1994.
[19] Julian J, Iskandar W, Wahyuni F, Nely Toding Bunga dan. Jurnal Asiimetrik: Jurnal Ilmiah Rekayasa Dan Inovasi Karakterisasi Efek Co-Flow Jet Sebagai Salah Satu Perangkat kontrol Article information 2022;4:185–92.
[20] Wang XK, Tan SK. Experimental investigation of the interaction between a plane wall jet and a parallel offset jet. Exp Fluids 2007;42:551–62. https://doi.org/10.1007/s00348-007-0263-9.
[21] THE PLANE TURBULENT FREE JET. n.d.

[22] Gu R, Member A. MODELING Two-DIMENSIONAL TURBULENT OFFSET JETS FIG. 1. Schematic of 20 Offset Jet PREVIOUS STUDIES AND PRESENT WORK. n.d.